Relative reactivity of oxygenated fuels: alcohols, aldehydes, ketons and methyl esters.

Journal:	*Energy & Fuels*
Manuscript ID	ef-2016-01171h.R1
Manuscript Type:	Article
Date Submitted by the Author:	n/a
Complete List of Authors:	Pelucchi, Matteo; Politecnico di Milano, Chemistry, Materials and Chemical Engineering Cavallotti, Carlo; Politecnico di Milano, Chimica, Materiali e Ingegneria Chimica Ranzi, Eliseo; politecnico, CMIC Frassoldati, Alessio; Politecnico di Milano, Chimica, Materiali e Ingegneria Chimica Faravelli, Tiziano; Politecnico di Milano, Chimica, Materiali e Ingegneria Chimica

Relative reactivity of oxygenated fuels: alcohols, aldehydes, ketons and methyl esters.

Matteo Pelucchi, Carlo Cavallotti, Eliseo Ranzi, Alessio Frassoldati, Tiziano Faravelli

Department of Chemistry, Materials and Chemical Engineering "G. Natta", Politecnico di Milano, P.zza Leonardo da Vinci 32, 20133 Milano, Italy

Abstract

This work aims at comparing and highlighting the main reaction pathways, characterizing the combustion behavior of oxygenated fuels. Ethanol and heavier alcohols are already viable biofuels, despite some concern on their aldehyde and ketone emissions. Recently, the potential of 2-butanone (methyl ethyl ketone) as anti-knocking fuel was investigated at engine relevant conditions. Moving from methyl butanoate, long chain fatty acid methyl esters are largely considered and used as biodiesels, mainly in Europe. Starting from a consistent assessment of C-H and C-C bond dissociation energies in *n*-butane, *n*-butanol, *n*-butanal, methyl-ethyl ketone and methyl butanoate, their impact on the selectivity of the different H-abstraction reactions and their relative reactivity is analyzed. Low temperature oxidation mechanism of 1-butanol and 2-butanone are also presented and discussed. Based on the upgraded Politecnico di Milano (POLIMI) kinetic mechanism, the relative reactivity of n-butane and the different oxygenated fuels is here deeply discussed. Stoichiometric fuel/air mixtures at 10 and 30 atm and 600-1450 K are analyzed. At low temperatures (T<675K), *n*-butanol and 2-butanone show the lowest reactivity whereas the other fuels tend to converge to a very similar behavior. *n*-butanal is the fastest to ignite in the whole T range, because of the weakest C-H bond dissociation energies. No NTC behavior is observed for *n*-butanal and *n*-butanol, under the investigated conditions. A weak NTC is predicted for methyl butanoate, similar to that of propane. Methyl butanoate and 2-butanone are the slowest to ignite between 750 K and 850 K. A limited number of fuel-specific reactions characterizing each fuel and deserving more accurate investigation is highlighted, together with the lack of experimental targets below 850 K for methyl butanoate and 2-butanone.

Keywords

Kinetic modeling

Bond dissociation energies

H-abstraction reactions

Low temperature kinetics

Biofuels

1. Introduction

Over the next few decades, population and income growth are expected to create new demands for energy. Particularly, rising prosperity will drive increased energy demand for transportation (~40% by 2040 [1]) Despite the decreasing trend of fossil fuels price [2, 3], government incentive programs [4], environmental issues (e.g. greenhouse gas emissions) and the need of lowering import dependency from political unstable countries [5], drive the exploitation of biofuels (e.g. alcohols) and biodiesels (e.g. methyl esters) for transport. In this context, as recently reported by Bergthorson and Thomson [6], fundamental combustion properties (i.e. chemical-kinetics) rule engine performances and exhaust pollutant emissions of advanced biofuels. Kinetic modeling advances the understanding of the influence of specific chemical compounds allowing the tailoring of a fuel, or fuel blend, for an existing engine technology or the tuning of an engine for a desired blend. As recently reviewed by Sarathy et al. [7], alcohols with different carbon number and substitution can be used in modern internal combustion engines with minor modifications to the engine design. Besides ethanol, which is nowadays conveniently produced from corn and sugar cane and widely used as a biofuel, other linear and branched alcohol species are foreseen as viable biofuels for road, air and sea transport. Some concern exists on pollution from alcohol fueled engines. Sadeghinezhad et al. [8] presented a statistical analysis on biofuels performances in terms of power, fuel economy and pollutants emissions. While PM, CO and HC emissions generally improve when a biofuel is used, a large increase in carbonyl compounds release is observed (aldehydes and ketones). Despite aldehydes formation

pathways during alcohols oxidation at low (~500-1000 K) and high temperatures (~1000-2500 K) are quite understood, very few kinetic modeling studies specifically addressing aldehydes exist in the literature [9-11].

The Cluster of Excellence "Tailored Made Fuels from Biomass" (TMFB) recently identified methyl ethyl ketone, together with 2-methylfuran, as promising future biofuels through an effective interdisciplinary approach [12]. Part of the activity in the TMFB was devoted to a better assessment of MEK anti-knocking properties from a kinetics perspective. New experimental data in rapid compression machine were measured and a kinetic mechanism covering also the low temperature conditions was developed [13].

Biodiesels are complex mixtures of multi-component alkyl esters of long-chain fatty acids, generally produced by transesterification of soy and rapeseed oil with methanol [14]. Many kinetic studies have addressed the kinetic features of methyl esters in the last 10 years [15, 16]. The kinetic characterization of methyl esters conveniently started from methyl-butanoate (MB) which, due to its small size, allowed a better understanding of the influence of the ester moiety by introducing a relatively small number of species in detailed kinetic mechanisms.

Despite the large amount of kinetic studies on oxygenated species, a systematic characterization of the influence of the oxygenated functional group on their relative reactivity is still lacking in the literature.

The complexity of gas phase kinetics, together with the high level of accuracy required, led to a steep increase in kinetic mechanism size, both in terms of reactions and species [17]. As emphasized by Carstensen and Dean [18] the manual creation of gas-phase reaction mechanisms is not only a tedious and time-consuming procedure, but it is also prone to errors and incompleteness. In the last 25 years, many algorithms have been developed to automatically generate reaction mechanisms [19-23]. To allow the implementation of a consistent set of reaction pathways and include physically meaningful kinetic parameters, reaction classes need to be clearly defined [24, 25] and rate rules needs to be established and revised based on fundamental properties [26, 27], obtained from experiments and/or theory. Once rate rules are defined the extension to heavier species becomes relatively simple [28]. As widely known and

firstly generalized in complex kinetic mechanisms by Dente et al. [19, 29], H-abstraction reactions play a key role in determining the reactivity of a fuel both during pyrolysis and oxidation. As discussed in Ranzi et al. [30], the evaluation of the rate constant of the generic

R·+R'-H=R-H+R'·

reaction, depends on the properties of the abstracting radical (R) and on the type of hydrogen to be abstracted. As an example, the activation energy required by an alkyl radical for a secondary H-atom abstraction in an alkane is lowered by ~2.5 kcal/mol with respect to the reference primary H-atom. Again, a tertiary H-atom abstraction is favored by ~4 kcal/mol. Whenever direct and more accurate kinetic parameters are not available, the automatic generation of H-abstraction reactions included in the global POLIMI mechanism [31] is based on these rules and energy corrections. The same approach is applied to oxygenated species where the presence of the oxygen atom largely influences the adjacent C-H and C-C bonds lowering their BDEs compared to alkane fuels.

This paper aims at providing a description of the main reaction pathways that characterize the reactivity of oxygenated fuels, as well as at identifying a rational interpretation of the kinetic motivations determining differences and similarities in the kinetic behavior of each fuels. In many cases, it is sufficient to refer to some key bond dissociation energies, which relates to few specific reaction channels. Despite the recent abundant literature on biofuels, this is the first attempt, to our knowledge, to investigate and rationalize the effect of the hetero O atom on the closest bond dissociation energies and, consequently, on the reactivity of straight chain fuels. Sudholt et al. [32] presented an analogous approach for furanic species emerging as promising biofuels from the TMFB project. The attempt of this previous study was to correlate the BDEs of saturated and unsaturated furans to their derived cetane number (DCN). Dominant H-abstraction channels were identified for every class of compounds, and the kinetic discussion was limited to the identification of successive decomposition or ring-opening reactions of the derived radicals. Insights on specific kinetic pathways were referred by analogy to previous studies for the high temperature oxidation of such compounds [32-34].

This study complements and differs from the previous approach [32] *i)* by analyzing the effect of four different functional groups (R-OH, R-(C=O)-H, R-(C=O)-R, R-(C=O)-O-CH_3) on BDEs and on fuel specific reaction pathways; *ii)* by providing a single kinetic mechanism able to quantify and reproduce the features of the different fuels; *iii)* by focusing the kinetic discussion on the low temperature oxidation, where the fuels mostly differ in terms of reactivity.

The discussion presented in this paper is mostly based on the general, hierarchical and lumped kinetic mechanism developed at Politecnico di Milano over the last 30 years, effectively serving the final goal of characterizing the different reactivity of oxygenated species. To this goal, the mechanism is extended to characterize the low temperature reactivity of n-butanol together with the low and high temperature reactivity of 2-butanone.

Section 2 of this paper provides a consistent assessment of the bond dissociation energies (BDEs) of the C-H and C-C bonds in *n*-butane, *n*-butanol, *n*-butanal, methyl-ethyl ketone and methyl butanoate (MB). The differences in BDEs justify the relative rate parameters of the H-abstraction reactions and their relative selectivity for oxygenated species, as included in POLIMI mechanism (Section 3). An updated and extended validation of *n*-butane and oxygenated species in the whole temperature range is presented in Section 4. Lastly, Section 5 summarizes and discusses the impact of different oxygenated functional groups on the reactivity (i.e. ignition delay time), from low to high temperatures.

2. Bond Dissociation Energies

The computational method G4 developed by Curtiss et al. [35] and implemented in the Gaussian-09 suite of programs [36] was adopted to calculate C-H and C-C bond dissociation energies. The G4 method has been proved to be within the most reliable to calculate thermochemistry and therefore BDEs [37].

According to the following reactions

R-H→R·+H· (for C-H bonds)

and

R-R'→R·+R' (for C-C bonds)

the BDEs are determined as the difference in the 298K G4-energy between the corresponding radical (·R) and H· (or ·R') and the parent compound (R-H or R-R'). All energies were computed with reference to the minimum energy structure using the rigid rotor harmonic oscillator approximation. To determine the minimum energy structure potential energy curves for internal rotation of single bonds for the parent and radical species were determined using the B3LYP/6-31+G(d,p) level of theory performing relaxed scans at 20° intervals. *Figure **1*** shows BDEs obtained in this study for *n*-butane, *n*-butanol, *n*-butanal, MEK and methyl butanoate at the G4 level and 298 K. *Figure **1*** also reports a Δ_{BDE} (parentheses) assuming the BDE of the primary C-H bond of butane as a reference. Calculated BDEs are in good agreement with those estimated with the MRACPF2 method by Oyeyemi et al. [38-40] with maximum deviations of ~2 kcal/mol as reported in Table S1 of the Supplemental Material. The calculated values are also compared with experimental values (brackets of Figure 1) when available [41, 42]. Maximum deviations from experimental values are ~1 kcal/mol. As the aim of this study is to provide a consistent set of BDEs to discuss the relative reactivity of oxygenated species with different functional groups, the obtained agreement is considered satisfactory.

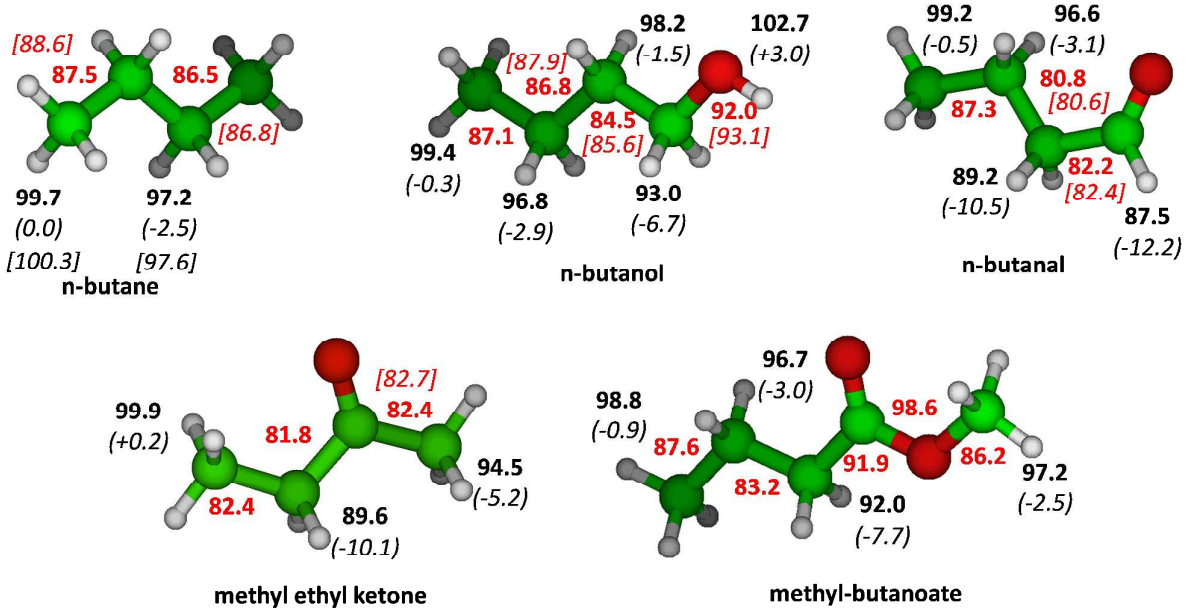

Figure 1: C-H (black) and C-C (red) bond dissociation energies (kcal mol^{-1}) for butane, n-butanol, n-butanal, methyl ethyl ketone and methyl butanoate calculated at the G4 level (298 K)[35]. Numbers in parentheses represent the difference in BDEs (Δ_{BDE}) with respect to a primary C-H bond. Numbers in brackets [ ] are experimental values [41, 42].

Electronegativity of the oxygen atom typically reduces the strength of the closest bonds. *n*-butanol and especially *n*-butanal and methyl ethyl ketone (MEK) show a reduced energy of both the alpha C-C bond and the beta C-H bond. On the contrary, the substituted carboxyl group of methyl-butanoate makes the molecule more stable. The mesomeric structures of unshared pair of electrons in the oxygen singly bonded to carbonyl carbon, allow the formation of the ester resonance, which stabilizes the molecule. Consequently, the close C-C bond results stronger with a high dissociation energy (~92 kcal/mol).

3. Selectivities of H-abstraction reactions

Coherently to the relative bond strengths discussed in Section 2, previous kinetic studies have adopted specific rate constants reflecting the effect of the presence of the oxygen atom in different functional groups. Beside C-C bond dissociation energies, whose values mainly affects the rate of radical chain initiation reactions, H-abstraction reactions dominate fuel consumption in the whole temperature range of interest for combustion systems (500-2000 K). While at low temperatures the abstracting radicals are typically OH and, to a lesser extent HO_2, at higher temperatures and particularly under pyrolysis or fuel rich conditions, also H and CH_3 become important H-abstracting radicals. Assuming that the rate of abstraction

largely depends on the nature of the H-atom to be abstracted, it is clear how intrinsic bond dissociation energies directly affect the rate values, and, more importantly, the relative selectivities of the available abstraction sites. Figure 2 shows the H-abstraction rates of primary, secondary, and tertiary H-atoms by H, OH and CH_3 radicals on a per H-atom basis, according to the generic rate rules [19]. Considering H-abstractions on *n*-butane by OH at 1000 K, the four available secondary H-atoms contribute to ~60% of the total rate constant, while ~40% undergoes a H-abstraction on the terminal methyl groups. According to Benson (Thermochemical Kinetics. 1979) and Carstensen and Dean [43], only short range forces affect the reaction rates, therefore the effect of the functional group vanishes after the β positions. This assumption is further confirmed by the values reported in Figure 1. Thus, the rate of H-abstractions from the terminal CH_3 group is taken as that for alkanes, with the exception of (the) MEK.

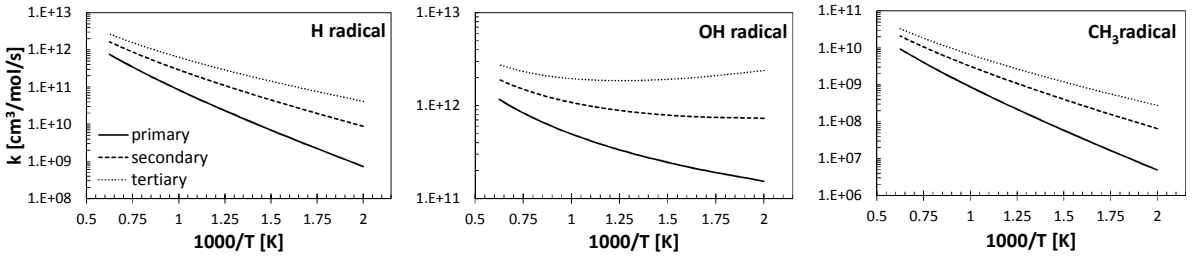

Figure 2: H-abstraction reactions. Calculated rate constants (per H-atom) for simple primary, secondary, tertiary H-atoms.

3.1 *n*-butanol

Figure 3 shows the relative selectivities of the H-abstraction reactions by OH radical of *n*-butanol at T=1000 K, as evaluated and discussed by Frassoldati et al. [44]. In agreement with the BDEs of *Figure **1***, the α position is the dominant one (~45%), followed by the alkane-like secondary position γ (~25 %). β position only contributes ~15%, due to its higher BDE (98.2 kcal/mol) compared to the one of the γ site.

According to the low temperature study of da Silva et al. [45] on the kinetics of the α-hydroxyethyl radical addition to O_2, R-·CH-OH radicals are assumed to interact with O_2 mainly producing HO_2 and the parent aldehyde (e.g. R-·CH-OH+O_2=HO_2+R-CHO). Thus, the formation of peroxy radicals from the predominant α radicals is a negligible low temperature branching pathway for alcohol fuels. This feature partially justifies

the anti-knocking properties of alcohols up to butanol isomers (Research Octane Number=98-117, Motor Octane Number=85-95 [7]), making them useful for use in spark ignition engines.

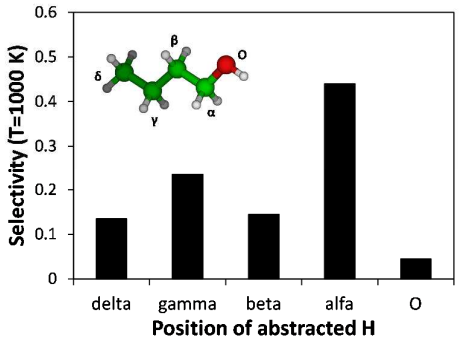

Figure 3: Selectivity of n-butanol radicals from H-abstraction reactions [44] by OH at T=1000 K.

3.2 *n*-butanal

Figure 4 shows the relative selectivities to the different positions in *n*-butanal oxidation according to the kinetic mechanism of Pelucchi et al. [9, 46] and of Veloo et al. [10].

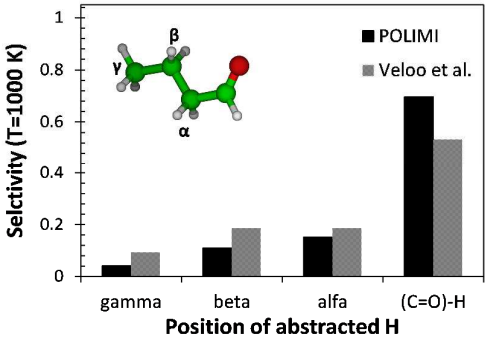

Figure 4: Selectivity of n-butanal radicals from H-abstraction reactions by OH at T=1000 K according to Pelucchi et al. [9, 46] (black bars), and Veloo et al. (striped bars) [10].

Despite some quantitative differences, both the mechanisms describe *n*-butanal oxidation as largely dominated (~50-70%) by H-abstraction at the weak C-H bond of the aldehydic site forming a carbonyl radical R_n-CO (i.e. C_3H_7CO). As recently discussed [46], carbonyl radicals heavier than acetyl do not add to oxygen, rapidly decomposing to CO and the corresponding alkyl radicals, whose low temperature branching pathways largely dominate aldehydes reactivity. Table 1 reports the branching ratios of the pseudo first order high pressure limit of C_3H_7CO addition to O_2 to form a carbonyl-peroxy radical, together with C_3H_7CO decomposition to CO and *n*-propyl radical. With regards to the bimolecular addition reaction, the pseudo

first order rate constant ($k_{app}=k_{add}[O_2]$) is based on the oxygen concentration of a stoichiometric *n*-butanal/air mixture (3.67% n-butanal/20.23% O_2/76.1% N_2) at 10 atm.

Because of the lower activation energy required for the decarbonylation (~15-16 kcal/mol) compared to that of the β-decomposition of alkyl radicals (~30 kcal/mol), the addition to O_2, activating the peracid channel, plays a role only at very low temperatures (T < 600 K).

Table 1: Branching ratios of C_3H_7CO addition to O_2 and its decomposition to CO and n-C_3H_7.

T [K]	C3H7·CO+O_2= C_3H_7CO-OO·	C3H7·CO=CO+·C_3H_7
400	1.00	0.00
500	0.85	0.15
600	0.22	0.78
700	0.03	0.97
800	0.01	0.99
900	0.00	1.00
1000	0.00	1.00

According to the BDEs of Figure 1, a significant selectivity of H-abstraction is expected for the secondary α position. With respect to the standard secondary H-atom in alkanes [30] a limited enhancing factor ~1.25 is applied, because of the resonantly nature of this stable radical, which inhibits reactivity from this channel.

3.3 methyl ethyl ketone

Figure 5 shows the relative selectivity of the three available abstraction channels in MEK, according to the rate constants proposed by Burke et al. [13] and to those adopted in this study (Section 4.4). The weakened secondary and primary C-H bonds, explain the predominant selectivity to α_s and α_p, accounting for ~50% and ~30% respectively.

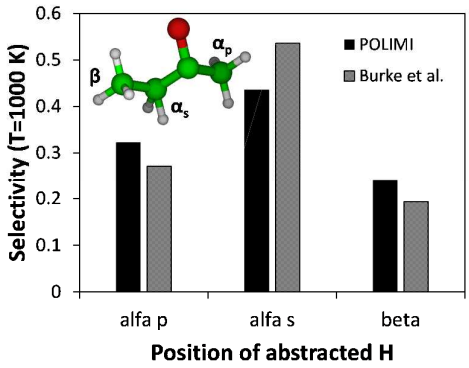

Figure 5: Selectivity of MEK radicals from H-abstraction reactions by OH at T=1000 K according to Burke et al. [13] and this study (POLIMI).

3.4 methyl butanoate

Grana et al. [47] already presented the high temperature oxidation mechanism of methyl butanoate (MB), together with a lumped low temperature mechanism derived from the detailed mechanism of Hakka et al. [48]. In a more recent study, Mendes et al. [49] calculated H-abstraction reactions by OH for a series of methyl esters (from methyl-etanoate to methyl-butanoate). Figure 6 shows the relative importance of H-abstraction channels according to the detailed mechanism of Hakka et al. [48], adopted in the mechanism, and according to the theoretical calculations [49].

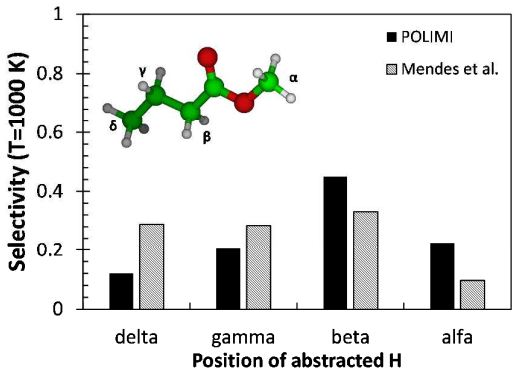

Figure 6: Selectivity of methyl butanoate radicals from H-abstraction reactions by OH at T=1000 K according to Hakka et al. [48] and Mendes et al. [49].

Again, Tan et al. [50] calculated H-abstraction reactions by important radicals (H, CH_3, OH, O, HO_2) for methyl-propanoate (MP). Figure 7 compares the experimental results for the total H-abstraction rate

constant by OH as measured by Lam et al. [51], with rate constants from recent theoretical studies [49, 50] and that included in the lumped POLIMI mechanism for methyl butanoate [47].

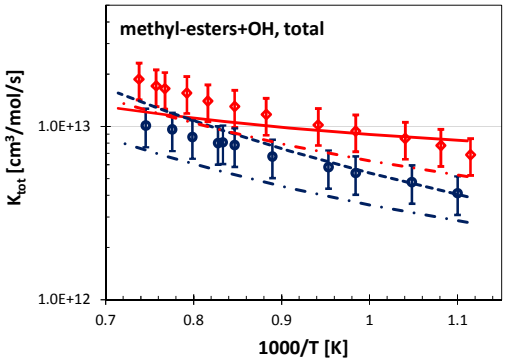

Figure 7: total rate constant for OH+MP (blue) and OH+MB (red). Symbols: experimental data by Lam et al. [51], solid line: POLIMI mechanism (MB) [47], dashed-dot line: Mendes et al. [49] (MP and MB), dashed line: Tan et al. [50] (MP).

Despite the overall agreement between rate constant estimates and/or calculation and experiments (factor of ~1.5), Figure 8 shows some incoherent trend. In fact, according to the rate constants calculated by Tan et al. [50], the relative importance of the H-abstraction channels in MP at 1000 K, does not reflect the hierarchy in BDEs. Despite the surprising trend, it has to be mentioned that the same rate constants were recently found to have a positive effect on MP laminar flames prediction [52].

The C-H secondary bond in β is the weakest [38-40] and, giving rise to the formation of a resonantly allylic-like radical, is expected to be the favored channel for H-abstractions, accounting for 45% of the selectivity in MB. According to the calculations of Mendes et al. [49], this value is expected to increase up to 60~% for MP. A BDE based approach in this case provides also a useful guidance to critically interpret theoretical calculations.

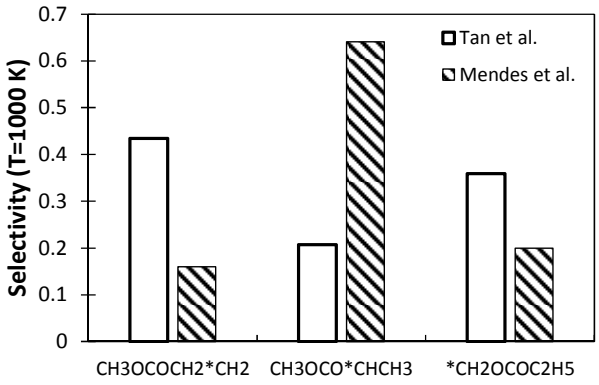

Figure 8: Selectivity of methyl propanoate radicals from H-abstraction reactions by OH at T=1000 K according to Tan et al. [50] and Mendes et al. [49].

Considering the low temperature oxidation, based on the length of the hydrocarbon chain in methyl butanoate and on the predominance of the H-abstraction from the central carbon β, typical negative temperature coefficient behavior is expected to be very limited, in agreement with observations of Gail et al. [53] and Walton et al. [54]. However, the analysis of the recent literature and the scarcity of data at temperatures lower than 800 K emphasize the uncertainty still existing in kinetic parameters for methyl esters.

4. Validation of the kinetic mechanisms of n-butane and oxygenated species

Before a kinetic analysis and discussion on the relative reactivity of n-butane and oxygenated fuels, a short validation of the updated kinetic mechanisms POLIMI_1605 is here presented. Moreover, the new lumped low temperature mechanisms of n-butanol and methyl ethyl ketone oxidation are also discussed. The global POLIMI mechanism includes ~500 species and ~20000 reactions, and is provided in the Supplemental Material attached to this study and on the website http://creckmodeling.chem.polimi.it/.

4.1 Lumped low temperature reactions

Due to the lack of symmetry in the molecular structure of oxygenated molecules, the size of the detailed kinetic scheme of pyrolysis and oxidation largely increases with respect to linear alkanes. Lumped or simplified approaches are therefore necessary to minimize the number of species and to allow easier extensions to longer species with the same functional group. An effective example of this systematic

generalization to heavier molecular weight compounds belonging to the same class, can be found in the sequential studies of Grana et al. [47, 55], recently successfully extended by Rodriguez et al. [56]. In the case of methyl-butanoate (see Section 4.6), a single alkyl-like radical was included to avoid exponential increase in the number of species when extending the kinetic mechanism to longer methyl-esters (C_{11}-C_{19} [55, 56]). For such fuels, detailed kinetic mechanisms from the literature can include up to ~5000 species, an order of magnitude more than the complete POLIMI mechanism.

Concerning the other oxygenated species analyzed in this study the detail of the different fuel radicals is maintained, allowing a more effective definition of site-specific reaction channels at high and low temperatures.

When generalizing this approach to oxidation reactions at low temperatures, it is necessary to include interactions of these radicals with O_2. Therefore, it is necessary to enlarge the kinetic scheme to include the intermediate lumped radicals RO_2, QOOH and its decomposition products (heterocyclic components and unsaturated species), OOQOOH, ketohydroperoxides, each one representing all the possible different isomers.

Following the validated and consolidated procedure proposed from more than 20 years by Ranzi et al. [20], the mechanism refers to only three intermediate lumped radicals (RO_2, QOOH, OOQOOH) and three stable species derived from the low temperature oxidation (cyclic component, unsaturated alcohol, aldehyde or ketone, ketohydroperoxide). Kinetic parameters of the lumped reactions (see Table 2 and Table 3) are derived by fitting the selectivities obtained with the lumped mechanism with those obtained with the detailed kinetic scheme defined upstream. The detailed kinetic scheme is implemented based on rate rules for standard low temperature reaction classes [27], taking into account site specific BDEs and fuel specific reaction classes for oxygenated fuels.

4.2 *n*-butane

n-butane kinetic mechanism [57] was recently revised with the inclusion of new reaction classes justifying the formation of organic acids and other minor oxygenated species at low temperatures [58]. Experiments

were performed in a Jet Stirred Reactor (JSR) by Herbinet et al. [59] at ~1.0 atm, for temperatures between 550 and 800 K, at a mean residence time of 6 s for a stoichiometric *n*-butane/oxygen/argon mixture (4/26/70 in mol%). Figure 9 shows a comparison of experimental data [59] with model predictions [58].

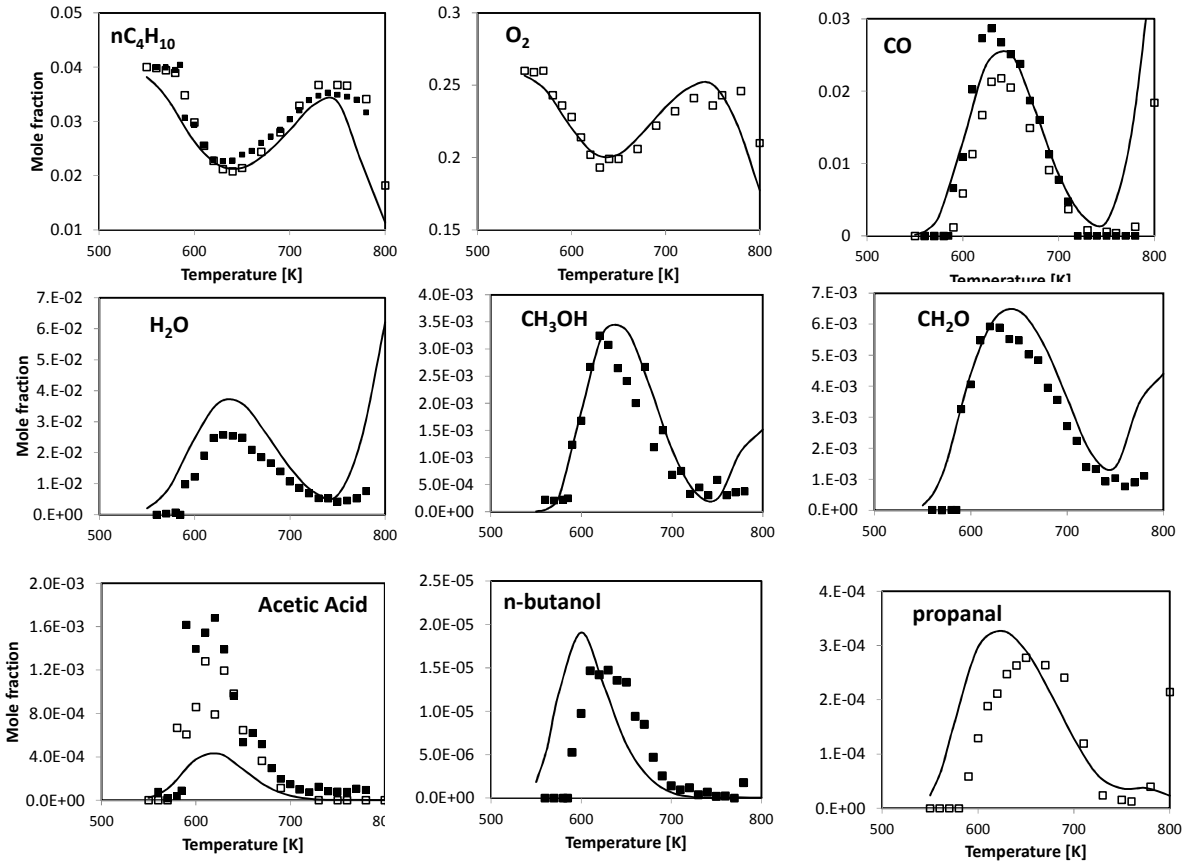

Figure 9: Oxidation of n-butane in jet stirred reactor (n-butane/O2/Ar = 4/26/70 mol%; 1 atm; residence time 6 s). Comparison of experimental measurements of Nancy (open symbols) and Hefei (full symbols) [59] with model predictions [58].

Predicted ignition delay times in shock tubes and rapid compression machines (RCMs) were measured by Healy et al. [60], between 1 and 40 atm. A comparison with mechanism predictions is given in Figure 10. To better highlight kinetic effects discussed in Section 5, RCM simulations were performed assuming an adiabatic constant volume reactor, not including heat losses. This simplification partially explains the observed deviations, as discussed in Cuoci et al. [61].

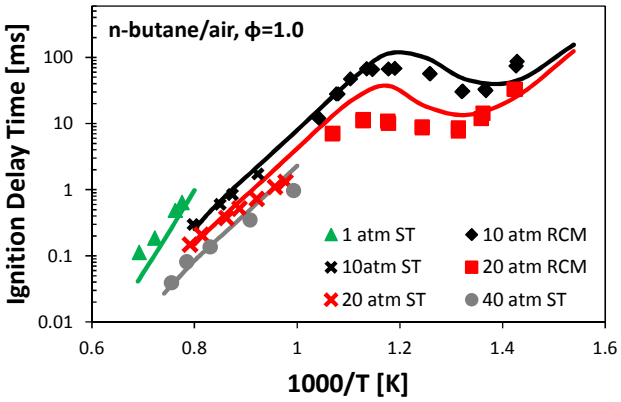

Figure 10: Ignition delay times of stoichiometrich n-butane/air mixtures. Experimental data by Healy et al. [60] (symbols) and model predictions [58].

4.3 *n*-butanol

The kinetic mechanism for butanol isomers was developed and extensively validated by Grana et al. [62] and partially revised later by Frassoldati et al. [44]. A lumped low temperature oxidation mechanism of n-butanol has been developed in this study and is reported in Table 2. Details of the lumped species representing the different isomers are reported in Table S2 of the Supplemental Material. Rate parameters are based on the low temperature rate rules by Ranzi et al. [27].

Table 2: Lumped low temperature reactions of n-butanol. Species: CH3CH2·CHCH2OH (β, secondary radical), CH3·CHCH2CH2OH (γ, secondary radical), ·CH2CH2CH2CH2OH (δ, primary radical) as in Figure 3. Lumped species: RBU1OOX (peroxy radicals), QBU1OOX (hydroperoxyalkyl radicals), ZBU1OOX (hydroperoxyalkyl peroxy radicals), KEHYBU1 (ketohydroperoxides), HCE-BU1 (hydroxyl cyclic ether). Units are cm^3, mol, s.

Reaction	A	E_a [cal/mol]
$CH_3CH_2{\cdot}CHCH_2OH+O_2 \rightarrow$RBU1OOX	2.50E+12	0
$CH_3{\cdot}CHCH_2CH_2OH+O_2 \rightarrow$ RBU1OOX	2.50E+12	0
$\cdot CH_2CH_2CH_2CH_2OH+O_2 \rightarrow$ RBU1OOX	2.50E+12	0
RBU1OOX $\rightarrow .3CH_3CH_2{\cdot}CHCH_2OH+.5$ $CH_3{\cdot}CHCH_2CH_2OH+.2{\cdot}CH_2CH_2CH_2CH_2OH+O_2$	3.00E+13	30000
RBU1OOX →QBU1OOX	4.50E+12	24000
QBU1OOX → RBU1OOX	5.00E+11	20000
QBU1OOX →HO_2 + unsat alcohol	2.00E+13	24000
QBU1OOX →OH+carbonyl+olefin/unsat alcohol	3.00E+13	24000
QBU1OOX →OH+HCE-BU1	1.00E+11	17000
O_2+ QBU1OOX → ZBU1OOX	2.50E+12	0
ZBU1OOX →O_2+ QBU1OOX	3.00E+13	30000
ZBU1OOX →OH+KEHYBU1	4.50E+12	24000
KEHYBU1→OH+$OHCH_2CHO$+CH_2CHO	5.00E+15	42000
RBU1OOX →OH+CH_2O+C_{n-1}aldehyde (Waddington)	1.00E+10	22000

Several experimental data allowed to validate this lumped mechanism. Ignition delay times were measured between 770-1250 K by Heufer et al. [63] and Vranckx et al. [64] at high pressure (10-80 bar). Rapid compression machine measurements were also presented by Weber et al. [65]. Figure 11 shows some comparisons between experimental data and results from adiabatic constant volume simulations. The kinetic mechanism, already extensively validated for high temperature conditions [44, 62], provides reliable results also at low temperatures and high pressures.

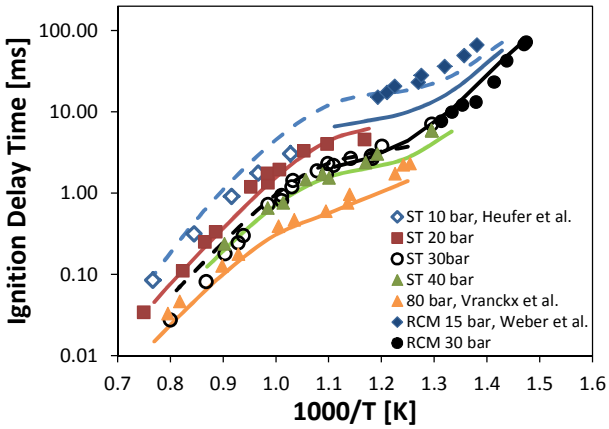

Figure 11: Ignition delay times of stoichiometrich n-butanol/air mixtures. Experimental data [63-65](symbols) and kinetic mechanism predictions (lines) (adiabatic constant volume simulations).

4.4 *n*-butanal

Pelucchi et al. [9] developed a kinetic mechanism for *n*-C_3-C_5 aldehydes pyrolysis and oxidation at high temperatures. The model was recently extended to describe the low temperature oxidation [46]. Figure 12 shows a comparison with the speciation data of Veloo et al. [10] in Jet Stirred Reactor at 10 atm, in the temperature range of 500-1100 K. Despite the slight underestimation of fuel conversion at low temperatures, the kinetic mechanism correctly predicts the effect of oxygen concentration and the extension of the NTC region. For the case at ϕ=0.5 a detailed comparison is reported, confirming the assumptions of the predominance of alkyl radicals low temperature chemistry, as discussed in Section 2 and more in detail in Pelucchi et al. [46].

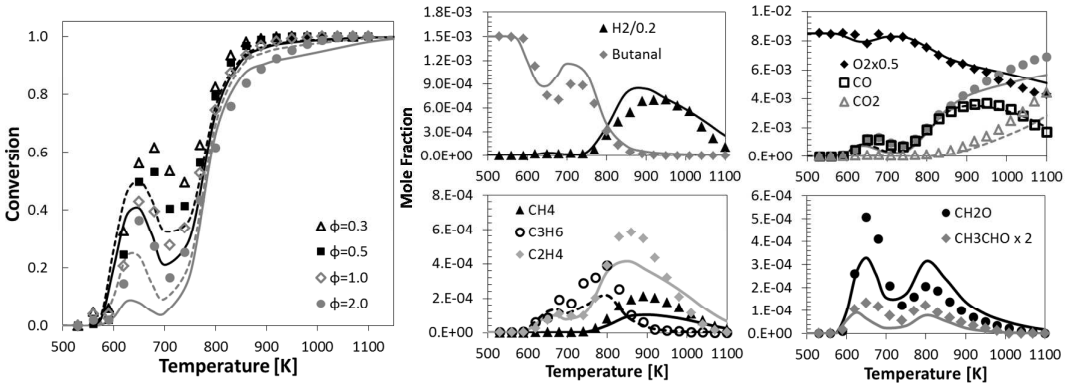

Figure 12: n-butanal (0.15%) oxidation in a JSR at 10 atm, τ=0.7 s. Fuel conversion for varying Φ and species profiles at Φ~0.5. Experimental data [10] (symbols) and mechanism predictions [46].

4.5 Methyl ethyl ketone

Methyl ethyl ketone (MEK) kinetics received large attention not only as an intermediate in hydrocarbon fuel combustion, but also for its role in the combustion of bio-oil from fast biomass pyrolysis [66-72]. The more recent work of Hoppe et al. [12] and Burke et al. [13] directly focused on its potential as biofuel. In particular Burke et a. [13] recently extended the available experimental data to conditions of interest for engines, measuring ignition delay times of MEK/air stoichiometric mixtures in rapid compression machine, between 850-1280 K, at 20 and 40 bar. Moreover, a kinetic mechanism including also the low temperature chemistry was developed and validated [13]. New experimental measurements were also carried out at the same conditions for a series of ketones [73] (acetone, 2-pentanone, 3-pentanone) at high temperatures (1028-1399 K) and high pressures (20 and 40 bar). Ignition delay time correlations were derived and the reactivity trend was explained based on BDEs, H-abstraction and radical decomposition reactions.

The high temperature pyrolysis and combustion mechanism of MEK is simply limited to the three main initiation reactions

$CH_3CH_2COCH_3 = CH_3CH_2\bullet + \bullet COCH_3$ $\qquad k = 2.\cdot 10^{16} \cdot \exp\left(-\frac{82500}{RT}\right) \qquad [s^{-1}]$

$CH_3CH_2COCH_3 = CH_3\bullet + \bullet CH_2COCH_3$ $\qquad k = 2.\cdot 10^{16} \cdot \exp\left(-\frac{84000}{RT}\right) \qquad [s^{-1}]$

$CH_3CH_2COCH3 = CH_3CH_2CO\bullet + \bullet CH_3$ $\quad k = 2.\cdot 10^{16} \cdot \exp\left(-\frac{84000}{RT}\right) \quad [s^{-1}]$

together with three possible H-abstraction channels:

$R\bullet + CH_3CH_2COCH_3 = RH + CH_3\bullet CHCOCH_3$ $\quad k^{OH} = 8.8 \cdot 10^5 \cdot T^2 \cdot \exp\left(\frac{2260}{RT}\right) \quad \left[\frac{cm^3}{mol \cdot s}\right]$

$R\bullet + CH_3CH_2COCH_3 = RH + CH_3CH_2CO\bullet CH_2$ $\quad k^{OH} = 1.6 \cdot 10^6 \cdot T^2 \cdot \exp\left(\frac{474}{RT}\right) \quad \left[\frac{cm^3}{mol \cdot s}\right]$

$R\bullet + CH_3CH_2COCH_3 = RH + \bullet CH_2CH_2COCH_3$ $\quad k^{OH} = 1.2 \cdot 10^6 \cdot T^2 \cdot \exp\left(\frac{474}{RT}\right) \quad \left[\frac{cm^3}{mol \cdot s}\right]$

While the H-abstraction reactions are written in their generic form for all the H-abstracting radicals (R•), rate parameters reported above specifically refer to OH as the abstracting radical. The first H-abstraction reaction (referred to as α_s in Figure 5 of Section 3) is the dominant one also at low and intermediate temperatures accounting for slightly more than the 50% of the total propagation rate and MEK depletion.

Burke et al. [13] adopted rate constants for H-abstraction by OH as calculated by Zhou et al. [74]. According to the authors, the overall uncertainty of these theoretical calculation is a factor of ~3.0, due to uncertainty in energy calculations, tunneling effects and hindered rotors treatment. Figure 13a shows a comparison between the total H-abstraction rate constant by OH in POLIMI mechanism, the experimental values of Lam et al. [69], and the total rate constant as calculated by Zhou [74]. Panel b to d, show a detailed comparison of the site-specific rate constant showing good agreement between the values adopted in POLIMI mechanism and theoretical calculations [74].

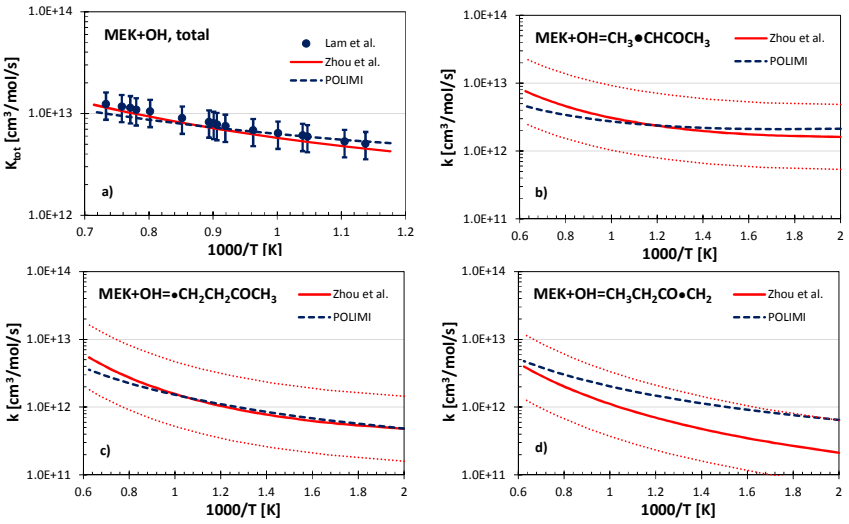

Figure 13: a) Total rate constant of OH+MEK. b-d) Site specific rate constant for H-abstraction by OH. Symbols: experimental data [69], red solid lines [74], red dotted lines: uncertainty (~2.5 as in [74]), black lines: POLIMI.

Lam et al. [70] studied the high-temperature pyrolysis of MEK behind reflected shock waves by using several species time-history measurements. Figure 14 shows comparisons between experimental data and model predictions.

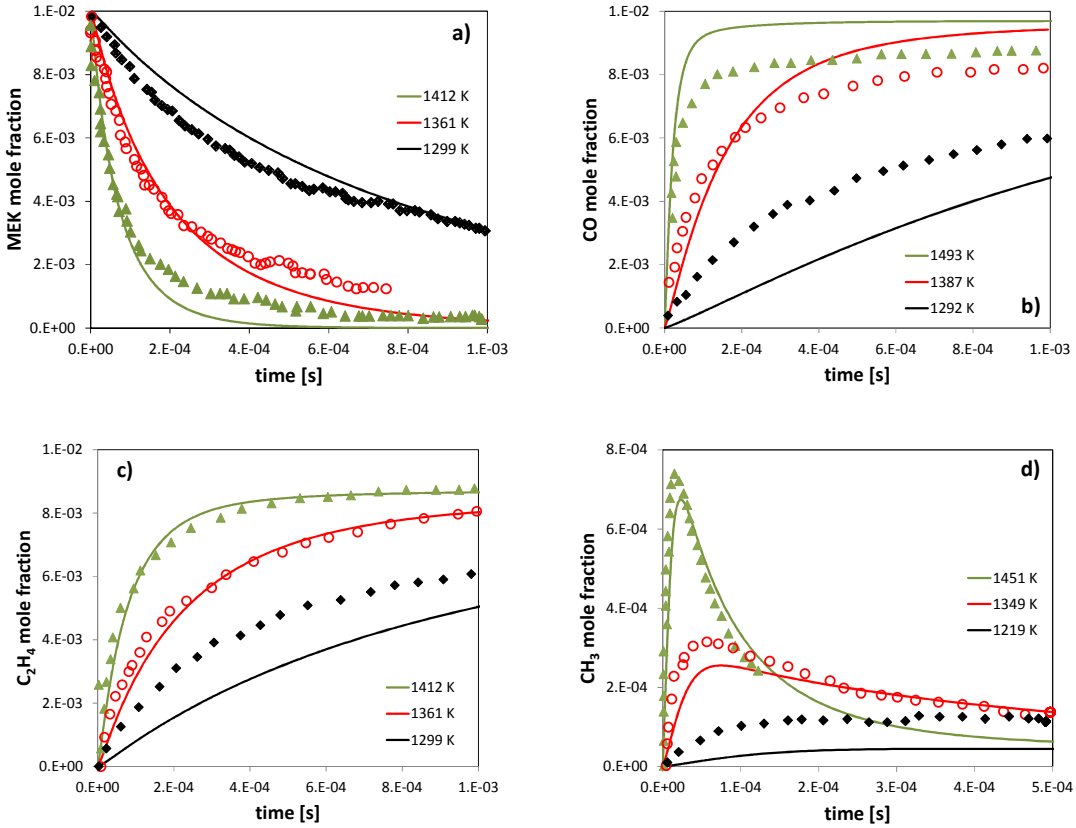

Figure 14: Pyrolysis of MEK. Panel a) Time-history of 1% MEK in Ar. Panel b) and c) time-histories of CO and C_2H_4 for 1% MEK in Ar. Panel d) time-history of methyl radical for 0.25% MEK in Ar. Comparisons of experimental data (symbols) [70] and model predictions (lines).

Recently, Badra et al. [71] presented shock tube ignition delay times of MEK ($C_2H_5COCH_3$) over temperatures of 1100–1400 K, pressures of 3–6.5 atm, at equivalence ratios of 0.5 and 1. They also modified the chemical kinetic mechanism of Serinyel et al. [72] improving MEK reactivity, because of systematic over-predictions of the ignition delay times, with respect to their experimental data. Figure 15 shows the satisfactory agreement of POLIMI mechanism predictions with these data, both in terms of pressure and stoichiometry dependence. On the contrary, the model systematically under-predicts the ignition delay times of Serinyel et al. [72] at least by a factor of two.

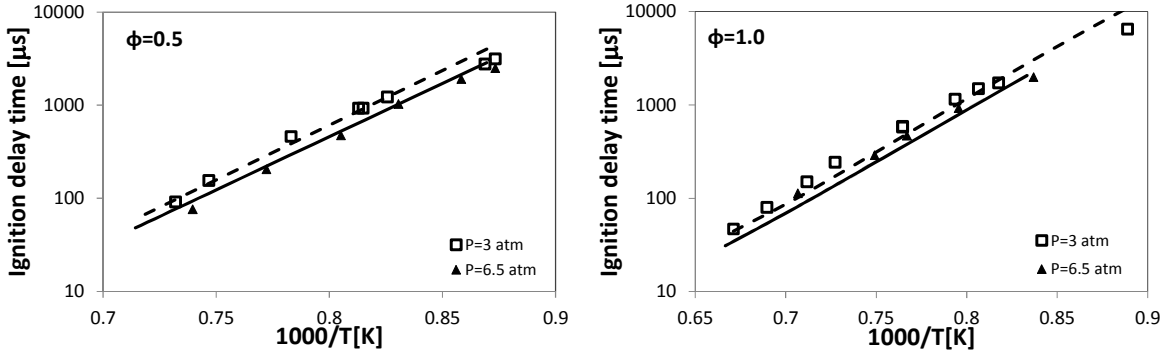

Figure 15: Ignition delay times for MEK/O_2/Ar mixtures at 3 and 6.5 atm (Φ= 0.5 and Φ= 1.0). Experimental data from Badra et al. [71].

The recent works of Hoppe et al. [12] and Burke et al. [13] highlighted the anti-knocking property and the lower reactivity of MEK with respect to commercial gasoline, in the temperature range 850-1000 K. From a kinetic perspective, the presence of the carbonyl group weakens the adjacent C-H bonds, and stabilizes both the alkyl radical and the peroxy radical formed via addition to O_2. The high rate of HO_2 elimination (mainly RMEKOO=>HO_2+CH3COCHCH2) largely explains the observed lower reactivity.

Burke et al. [13] reported a detailed discussion on RMEKOO=>HO_2+CH3COCHCH2 (methyl vinyl ketone), based on previous studies [67, 75]. These literature values were found to largely differ from each other (i.e. factor of ~7). Figure 16 shows a comparison of the rate constant adopted in the lumped mechanism, and those adopted in previous studies on MEK [13] and diisopropyl ketone (DIPK) [75], weighted on the relative abundance of α_s and β radicals in each mechanism. The lumped rate constant is respectively ~1.6 and ~2.0

times faster than the literature values. As in the lumped approach RMEKOO represents all of the peroxy radical isomers in MEK oxidation, the comparison is carried out by weighing the rate constants in the detailed mechanisms by the relative abundance of the two radicals (α_s and β) leading to this pathway, i.e. the selectivity to their formation as a function of temperature.

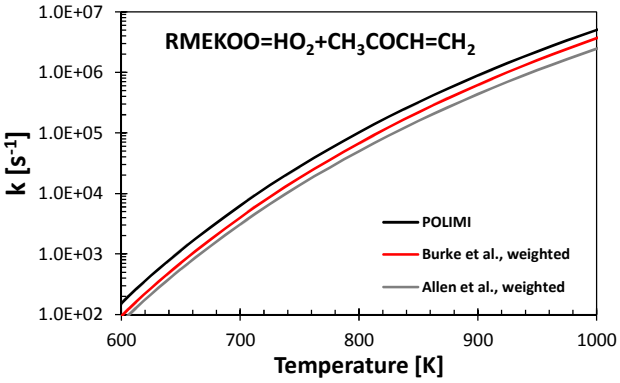

Figure 16: Comparison between the lumped rate constant for RMEKOO=>HO2+CH3COCHCH2 and the rate constants adopted in previous detailed kinetic mechanism [13, 75].

Beside the above reaction, the total number of available H-atoms for the internal isomerization to form the lumped hydroperoxy alkyl radical (RMEKOO=>QOOH-MEK) is lower than in *n*-butane. The coupling of the two effects leads to a prevalence of chain propagating reactions with respect to chain branching reactions typical of the low temperature oxidation of alkanes [12, 13].

The lumped low temperature oxidation mechanism of MEK, as developed in this study, is reported in Table 3. Details of the lumped species representing the different isomers are reported in Table S2 of the Supplemental Material. Figure 17 compares constant volume simulations with the recent experimental data of Burke et al. [13] and shows the weak effect of the low temperature reactions, in these conditions.

Table 3: Lumped low temperature reactions of methyl ethyl ketone. Species: RMEKAS (α, secondary radical), RMEKAP (α, primary radical), RMEKB (β, primary radical) as in Figure 5. Lumped species: RMEKOO (peroxy radicals), QOOH-MEK (hydroperoxyalkyl radicals), OOQOOH-MEK (hydroperoxyalkyl peroxy radicals), KHYMEK (ketohydroperoxides), CCE-MEK (carbonyl cyclic ether). Units are cm^3, mol, s.

Reaction	A	E_a [cal/mol]
RMEKAS+O_2→RMEKOO	2.00E+12	0
RMEKAP+O_2→RMEKOO	2.00E+12	0
RMEKB+O_2→RMEKOO	2.00E+12	0
RMEKOO→.5RMEKAS+.3RMEKAP+.2RMEKAB+O_2	2.00E+13	28000
RMEK+O_2↔HO_2+$CH_3COCH=CH_2$	2.50E+12	6000
RMEKOO→HO_2+$CH_3COCH=CH_2$	3.00E+13	31000

RMEKOO→QOOH-MEK	1.00E+12	26000
QOOH-MEK→RMEKOO	1.00E+10	16000
QOOH-MEK→HO_2+$CH_3COCH=CH_2$	2.00E+11	21000
QOOH-MEK→OH+CH_2CO+CH_3CHO	5.00E+13	22500
QOOH-MEK→OH+CCE-MEK	2.00E+11	16700
O_2+QOOH-MEK →OOQOOH-MEK	5.00E+12	0
OOQOOH-MEK→O_2+QOOH-MEK	2.00E+13	28000
OOQOOH-MEK→OH+KHYMEK	1.00E+12	26000
KHYMEK→OH+CH_2O+CO+CH_3CO	3.00E+15	43000
KHYMEK→OH+CH_2O+CH_2CO+HCO	2.00E+15	43000

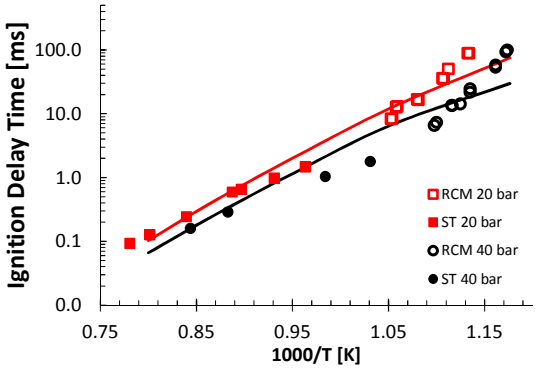

Figure 17: Ignition delay times of stoichiometrich MEK/air mixtures. Experimental data [13] (symbols) and kinetic mechanism predictions (lines) (adiabatic constant volume simulations).

4.6 Methyl butanoate

Grana et al. [47] extensively investigated the oxidation of methyl butanoate in shock tubes, plug flow reactors, jet stirred reactors, rapid compression machines and premixed laminar flames. For the low temperature oxidation a lumped kinetic mechanism mostly based on the work of Hakka et al. [48] was developed. Model predictions are compared to the ignition delay time measurements of HadjAli et al. [76] at T=815 K, Φ=1.0 and varying compressed pressure in RCM in Figure 18.

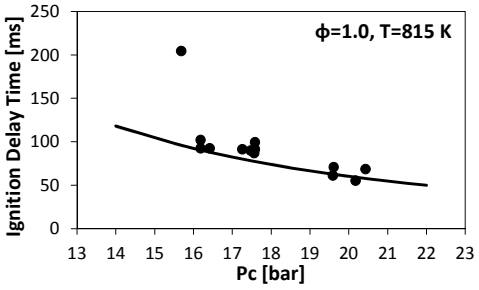

Figure 18: Ignition delay times of stoichiometric methyl butanoate/air mixtures at T=815 K and varying compressed pressure. Experimental data [76](symbols) and model predictions (lines) [47].

As a further comparison, Figure 19 shows species profiles measured by Gail et al. [77] in atmospheric JSR, in the temperature range of 850-1400 K, at ϕ=0.75 and residence time of 0.07 s.

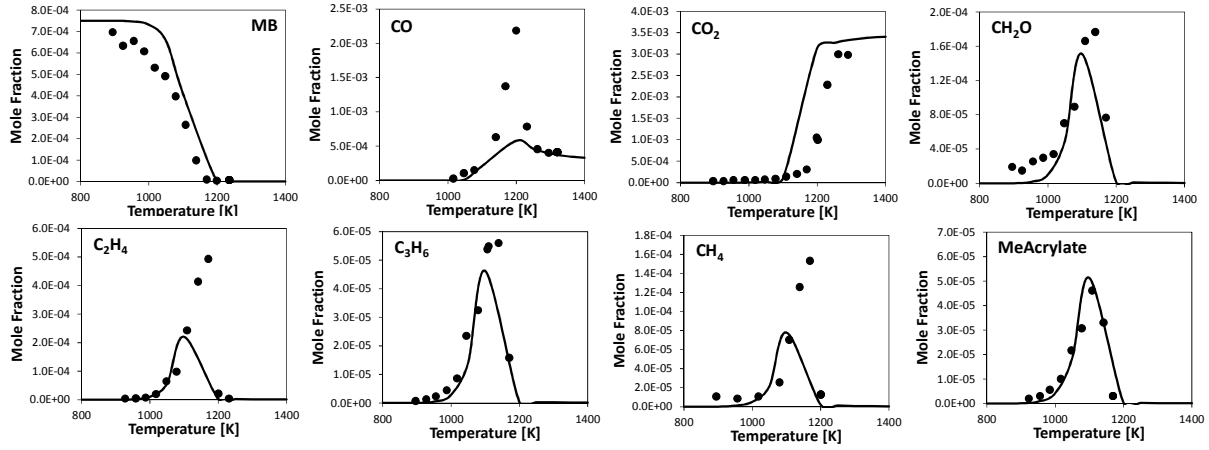

Figure 19: Experimental results [77] and model predictions [47] of major products from methyl butanoate oxidation in the JSR at φ=0.75, atmospheric pressure and 0.07 s.

5. Relative reactivity of oxygenated fuels and the influence of the oxygenated moiety

Figure 20 compares the reactivity of *n*-butane, *n*-butanol, *n*-butanal, methyl ethyl ketone and methyl butanoate in terms of ignition delay times of stoichiometric fuel/air mixtures at 10 (a) and 30 atm (b and c). Considering that the relative reactivity of the fuels is very consistent at both pressures, the discussion will focus on the 10 atm case, where the differences at lower temperatures are clearer. In fact, as the pressure increases, the peroxy radical (RO_2) can better stabilize allowing more efficient isomerization reactions to form hydroperoxyalkyl radicals (QOOH). However, the fuel specific reaction pathways discussed in the following, directly derived from the effect of the different functional group on BDEs, still play a major role and explain the consistent trend observed in panel c of ***Figure 20***.

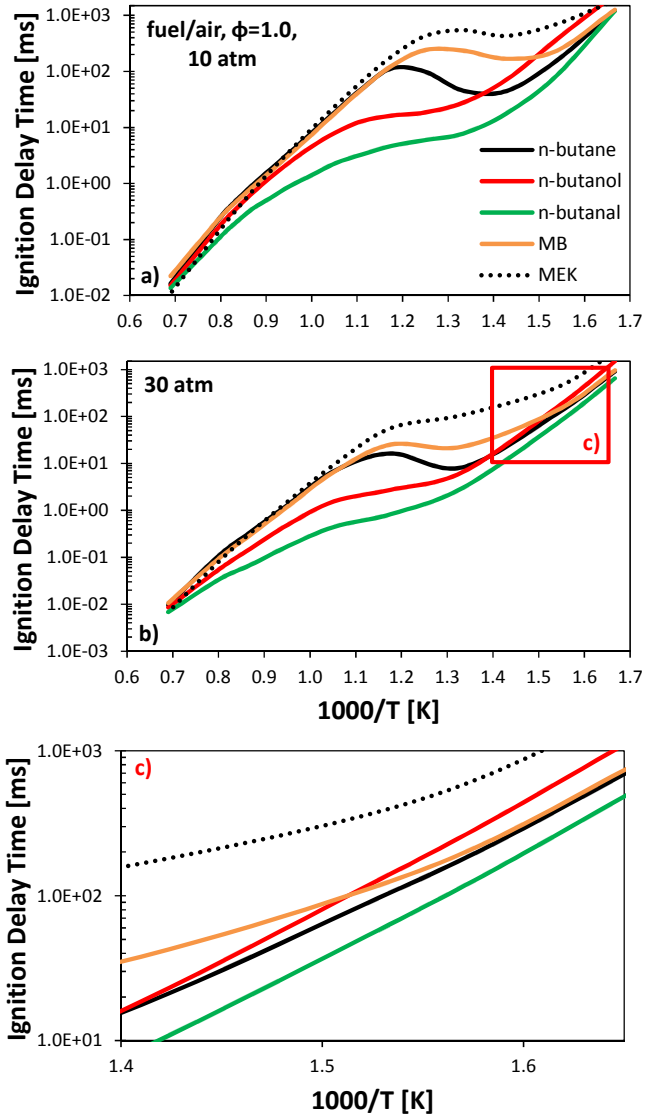

Figure 20: Relative reactivity of alkanes and oxygenated species. Ignition delay times of stoichiometric fuel/air mixtures at 10 atm (a) and 30 atm (b and c).

At high temperatures, the fuel pyrolysis controls the reacting process. The fast molecule decomposition forms components of lower molecular weight, which in turn oxidize. Thus, fuels behave quite similarly at these conditions. The initiation reactions play a significant role and this explains the slightly higher reactivity of *n*-butanol and especially of *n*-butanal. As shown in *Figure 1*, the oxygen atom weakens the closest C-C bonds, reducing their BDEs. In particular, the carbonyl group of *n*-butanal decreases the energies of both the nearest C-C bonds of about 5.5 kcal/mol, with respect to the corresponding bonds in *n*-butane. The hydroxyl group of *n*-butanol shows a lower weakening effect and affects the closest C-C bond

only, reducing its energy of about 3.6 kcal/mol, compared to the analogous bond between a primary and a secondary C atom of a linear alkane.

At low and very low temperatures (< 650 K), the typical branching decomposition reactions, via successive oxygen additions to radicals, and isomerization reactions leading to ketohydroperoxides are the prevalent pathways. Therefore, the induction times of *n*-butane, *n*-butanal and MB converge.

On the contrary, the low reactivity of *n*-butanol, that is its longer induction time, is due to the favored formation (~45% of fuel consumption) of the alpha radical ($CH_3CH_2CH_2{\cdot}CHOH$), because of the reduced BDE of the alpha C-H bond induced by the OH group (Figure 21). Once formed, the alpha radical does not undergo the typical low temperature branching mechanism, but it mostly produces *n*-butanal and HO_2 ($O_2+CH_3CH_2CH_2{\cdot}CHOH=C_3H_7CHO+HO_2{\cdot}$). Heufer et al. [78] obtained similar trends when comparing *n*-C_4-C_5 alcohols and alkanes reactivity at low temperatures.

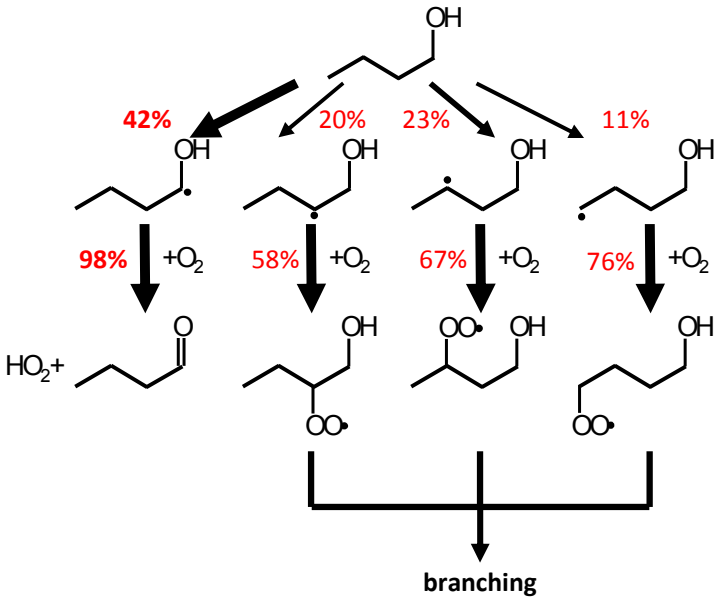

Figure 21: Sketch of the low T mechanism of n-butanol at 650 K and 10 atm. Pathways involving the butoxy radical (RO·), accounting for ~4% of n-butanol consumption and not contributing to the low temperature branching, have been omitted for clarity.

Also MEK is slow to ignite at T<800 K. Despite the HO_2 elimination from the peroxy radical could explain this behavior, additional experimental data in that specific temperature regime are needed for a better assessment of MEK low temperature reactivity.

The largest differences among the different fuels are observed at intermediate temperatures (750-950 K). **Error! Reference source not found.** shows the sensitivity analysis of the ignition delay times performed for the different fuels at stoichiometric conditions at 850 K and 10 atm. H-abstraction reactions, mainly by HO_2, are the activating reactions, together with the low/intermediate temperature mechanism, involving in particular additions to oxygen ($R+O_2$) and the peroxy radical isomerizations (RO_2=QOOH). Hydroperoxyalkyl radical (QOOH) decomposition to form HO_2 and the conjugate unsaturated species shows the most inhibiting effect, because of the relative stability of the hydroperoxy radical (HO_2).

n-butanal shows the lowest ignition delay times. The faster rate of H-abstraction from the aldehydic site, caused by the low BDE of the C-H bond (see Figure 1), justifies this higher reactivity with respect to the corresponding alkanes, alcohols and esters. Due to the fast decomposition of the carbonyl radical previously discussed [46], *n*-propyl radical low temperature oxidation dominates the reactivity of the aldehyde.

Second fastest fuel in these conditions is *n*-butanol. The low BDE of the alpha hydrogen results in a reduction of the reactivity, as reported in the sensitivity analysis of **Error! Reference source not found.**. The formed radical ($CH_3CH_2CH_2$·CHOH) does not undergo the conventional low temperature branching pathway, but interacts with O_2 forming the parent aldehyde and the less reactive HO_2 radical. All the other H-abstraction in β, γ and δ positions promote *n*-butanol reactivity, being γ the most favored position (see *Figure **3***).

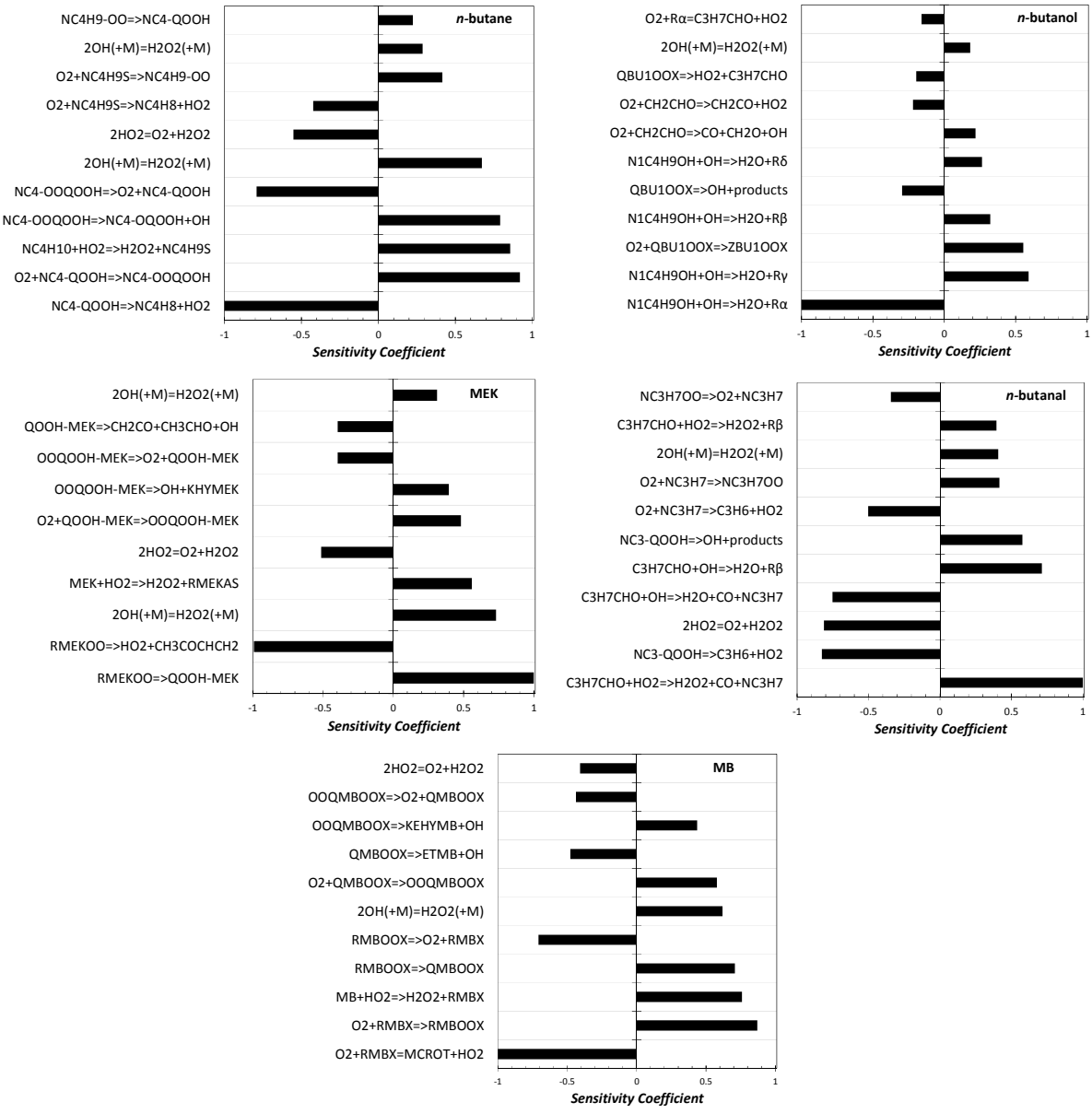

Figure 22: Sensitivity of ignition delay times to rate constants at 10 atm and 850K, for stoichiometric fuel/air mixtures. A positive sensitivity coefficient stands for a reaction increasing reactivity (i.e. decreasing ignition delay time). Sensitivity coefficient are normalized to +1/-1. For lumped species representing the different isomers refer to Table S2 in the supplementary material.

At intermediate temperatures, **Error! Reference source not found.** clearly shows that MEK limited reactivity is controlled by the very sensitive decomposition reaction of the peroxy radical RMEKOO to form HO_2 and methyl-vinyl-ketone.

The high production of HO_2 radical enhances its importance as abstracting radical from the weak C-H in α_s, giving rise to H_2O_2. The subsequent dissociation of hydrogen peroxide (H_2O_2+M=OH+OH+M) partly explains the positive sensitivity coefficient of H-abstraction by HO_2. It is clear that a correct assessment of HO_2 production via RO_2=>HO_2+unsaturated ketones and HO_2 consumption via H-abstraction is key in properly predicting MEK reactivity at these conditions. Figure 23 shows the main reaction pathway of MEK oxidation at 850 K and 10 atm.

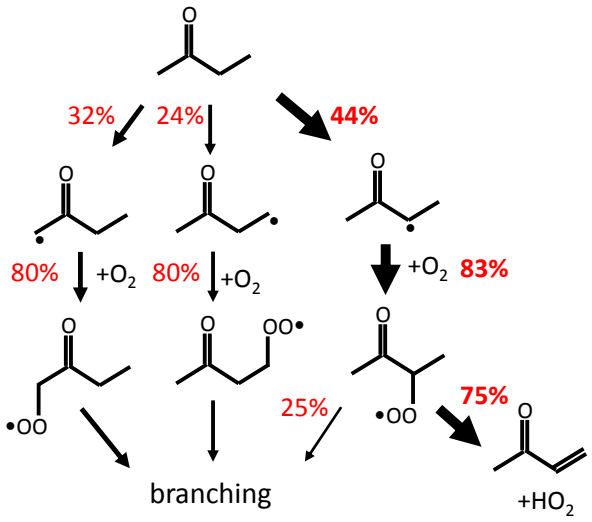

Figure 23: Relative importance of reaction pathways in methyl ethyl ketone (MEK) oxidation at 850 K and 10 atm.

Methyl butanoate (MB) lacks a pronounced NTC and shows the second slowest reactivity in the intermediate temperature range. Alpha C-H bond is weaker than those of *n*-butanol and *n*-butane, positively contributing to the reaction propagation. The stabilization resonance of the formed radical inhibits the successive oxygen addition. Moreover, the corresponding α-peroxy-methyl-butanoate radical can only isomerize, either through a seven membered ring or through a five membered ring (Figure 24). Both these paths are less favored, one for entropic reasons (too many rotors to block in the larger ring) and the other for energy reasons (extra strain of the 5-atom ring). Thus, as the sensitivity analysis of **Error! Reference source not found.** shows, the most effective reaction between oxygen and the alpha resonant radical is not the addition, but mainly the formation of HO_2 and the unsaturated methyl-crotonate (O2+RMBX=HO2+MCROT) [41], with the consequent decrease in reactivity.

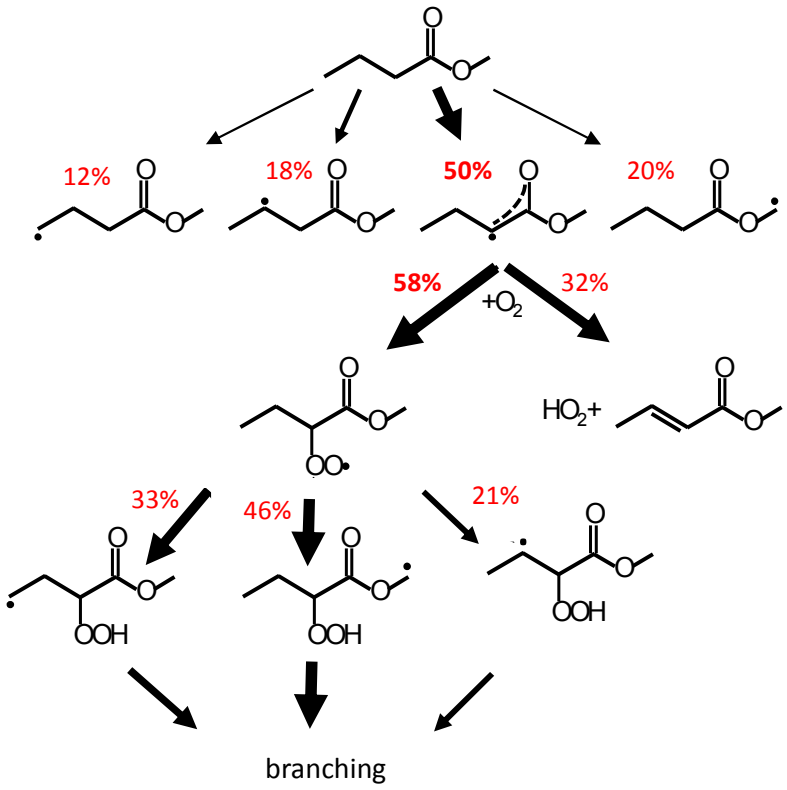

Figure 24: Sketch of main reactions the low T mechanism of methyl-butanoate (MB) at 850 K and 10 atm.

6. Conclusions

This work allowed the first comparative analysis of the reactivity of oxygenated fuels with different functional groups (R-OH, R-CHO, R-(C=O)-O-CH3, R-(C=O)-R).

A consistent assessment of C-H and C-C BDEs in *n*-butane and oxygenated species such as *n*-butanol, *n*-butanal, methyl ethyl ketone (MEK) and methyl butanoate (MB) has been provided, and they clearly reflect the effect of the oxygen molecule in different functional groups on the neighboring bonds.

Rate parameters of H-abstraction and initiation reactions implemented in the POLIMI mechanism, take into account these BDEs. The relative reactivity and selectivity of the H sites in the different fuels are also discussed. The upgraded POLIMI kinetic mechanism, here extended to the low temperature mechanisms of n-butanol and to the high and low temperature oxidation of MEK, is applied to support this kinetic analysis of relative reactivity of oxygenated species in the whole temperature range 600-1450 K.

In general, the reactivity scales as:

n-butanal > *n*-butanol > *n*-butane > MB > MEK.

The extreme reactivity of the aldehydic moiety leading to the formation of the carbonyl radical (C_3H_7CO) largely explains *n*-butanal ignition properties. Despite some secondary products from rather unknown and challenging reaction channels have been identified for longer aldehydes [79], it is quite understood that the major role at low temperatures is played by *n*-C_3H_7 branching pathways [46]. Ignition measurements for aldehydes at low temperatures would be useful to support such analysis.

At low temperatures (T<675K) *n*-butanol shows the lowest reactivity, because the favored α-radical mainly interacts with O_2 producing HO_2 and *n*-butanal, thus inhibiting the low temperature paths. As already pointed out by Sarathy et al. [7], very little information exist for the rate coefficient of this key reaction channel for linear alcohols longer than ethanol. A systematic theoretical analysis of this reaction class for a series of linear alcohols would be useful in defining an accurate rate rule.

Between 750 K and 850 K MEK and MB are the slowest to ignite. These results are consistent with those reported by Lin et al. [80] for MB. The lower reactivity is due to the sensitive peroxy radicals decomposition reactions to form HO_2 and, in the case of MB, mainly for the direct bimolecular reaction to form methyl crotonate (RMBX+O_2=HO_2+MCROT). Only one theoretical study focused on RMEKOO=HO_2+$CH_3COCH=CH_2$ [67], while no study addressed HO_2 formation in MB from these two channels. Despite recent extension of MEK experimental database [13], data below 850 K are still missing.

Above 1000 K, *n*-butanol ignition behaves similar to that of n-butane, MEK, and MB, whereas only at higher temperatures the fast ignition of *n*-butanal approach the common asymptotic behavior.

Sensitivity and flux analyses clarify how the presence of the oxygen atom, influencing closest bonds dissociation energies, activates specific reaction pathways, explaining the observed trends. Although the relative importance of H-abstraction sites seems quite understood and shared, the combustion kinetics community should systematically tackle the correct evaluation of the specific rate constants here

highlighted. Despite theoretical methods are now viable at affordable costs for relatively small molecules [81] (5-7 heavy atoms), these rate constants still carry relatively high uncertainties.

7. Acknowledgements

The authors gratefully acknowledge Prof. Mario Dente for helpful discussion. This work has been partially supported by the European Union's Horizon 2020 research and innovation programme (Residue2Heat project, G.A. No 654650). This work was strongly encouraged by the "CleanAir2015 Conference" Organizing Committee.

8. References

1. Exxonmobil, in: *The Outlook for Energy: A View to 2040*, Exxonmobil, (Ed.) 2015.
2. US Energy Information Administration. http://www.eia.gov/petroleum/gasdiesel/
3. IATA International Air Transport Association. http://www.iata.org/publications/economics/fuel-monitor/Pages/price-analysis.aspx
4. EU, in: EU, (Ed.) 2009; Vol. EUR-Lex - 32009L0028 - EN. http://eur-lex.europa.eu/legal-content/EN/ALL/?uri=CELEX%3A32009L0028.
5. A. Ajanovic; R. Haas, *Economic challenges for the future relevance of biofuels in transport in EU countries*, Energy 35 (8) (2010) 3340-3348
6. J. M. Bergthorson; M. J. Thomson, *A review of the combustion and emissions properties of advanced transportation biofuels and their impact on existing and future engines*, Renewable and Sustainable Energy Reviews 42 (2015) 1393-1417
7. S. M. Sarathy; P. Oßwald; N. Hansen; K. Kohse-Höinghaus, *Alcohol combustion chemistry*, Progress in Energy and Combustion Science 44 (2014) 40-102
8. E. Sadeghinezhad; S. Kazi; F. Sadeghinejad; A. Badarudin; M. Mehrali; R. Sadri; M. R. Safaei, *A comprehensive literature review of bio-fuel performance in internal combustion engine and relevant costs involvement*, Renewable and Sustainable Energy Reviews 30 (2014) 29-44
9. M. Pelucchi; K. P. Somers; K. Yasunaga; U. Burke; A. Frassoldati; E. Ranzi; H. J. Curran; T. Faravelli, *An experimental and kinetic modeling study of the pyrolysis and oxidation of n-C 3 C 5 aldehydes in shock tubes*, Combustion and Flame 162 (2) (2015) 265-286
10. P. S. Veloo; P. Dagaut; C. Togbé; G. Dayma; S. M. Sarathy; C. K. Westbrook; F. N. Egolfopoulos, *Experimental and modeling study of the oxidation of n-and iso-butanal*, Combustion and Flame 160 (9) (2013) 1609-1626
11. P. S. Veloo; P. Dagaut; C. Togbe; G. Dayma; S. Sarathy; C. K. Westbrook; F. N. Egolfopoulos, *Jet-stirred reactor and flame studies of propanal oxidation*, Proceedings of the Combustion Institute 34 (1) (2013) 599-606
12. F. Hoppe; U. Burke; M. Thewes; A. Heufer; F. Kremer; S. Pischinger, *Tailor-Made Fuels from Biomass: Potentials of 2-butanone and 2-methylfuran in direct injection spark ignition engines*, Fuel 167 (2016) 106-117
13. U. Burke; J. Beeckmann; W. A. Kopp; Y. Uygun; H. Olivier; K. Leonhard; H. Pitsch; K. A. Heufer; *A comprehensive experimental and kinetic modeling study of butanone*. Combustion and Flame (2016), in press.
14. A. Demirbas, *Progress and recent trends in biofuels*, Progress in Energy and Combustion Science 33 (1) (2007) 1-18

15. L. Coniglio; H. Bennadji; P. A. Glaude; O. Herbinet; F. Billaud, *Combustion chemical kinetics of biodiesel and related compounds (methyl and ethyl esters): Experiments and modeling–Advances and future refinements*, Progress in Energy and Combustion Science 39 (4) (2013) 340-382
16. J. Y. Lai; K. C. Lin; A. Violi, *Biodiesel combustion: advances in chemical kinetic modeling*, Progress in Energy and Combustion Science 37 (1) (2011) 1-14
17. T. Lu; C. K. Law, *Toward accommodating realistic fuel chemistry in large-scale computations*, Progress in Energy and Combustion Science 35 (2) (2009) 192-215
18. H.-H. Carstensen; A. M. Dean, *Rate Constant Rules for the Automated Generation of Gas-Phase Reaction Mechanisms†*, The Journal of Physical Chemistry A 113 (2) (2008) 367-380
19. M. Dente; S. Pierucci; E. Ranzi; G. Bussani, *New improvements in modeling kinetic schemes for hydrocarbons pyrolysis reactors*, Chemical engineering science 47 (9) (1992) 2629-2634
20. E. Ranzi; T. Faravelli; P. Gaffuri; A. Sogaro, *Low-temperature combustion: automatic generation of primary oxidation reactions and lumping procedures*, Combustion and flame 102 (1) (1995) 179-192
21. J. W. A. W. H. Green, B. A. Buesser, R. W. Ashcraft, G. J. Beran, C. A. Class, C. Gao, C. F. Goldsmith, M. R. Harper, A. Jalan, M. Keceli, G. R. Magoon, D. M. Matheu, S. S. Merchant, J. D. Mo, S. Petway, S. Raman, S. Sharma, J. Song, Y. Suleymanov, K. M. Van Geem, J. Wen, R. H. West, A. Wong, H.-W. Wong, P. E. Yelvington, N. Yee, J. Yu RMG - Reaction Mechanism Generator v4.0.1. http://rmg.sourceforge.net/
22. V. Warth; F. Battin-Leclerc; R. Fournet; P.-A. Glaude; G.-M. Côme; G. Scacchi, *Computer based generation of reaction mechanisms for gas-phase oxidation*, Computers & chemistry 24 (5) (2000) 541-560
23. S. Pierucci; E. Ranzi, *A review of features in current automatic generation software for hydrocarbon oxidation mechanisms*, Computers & Chemical Engineering 32 (4) (2008) 805-826
24. H. Curran; P. Gaffuri; W. J. Pitz; C. K. Westbrook, *A comprehensive modeling study of n-heptane oxidation*, Combustion and Flame 114 (1) (1998) 149-177
25. E. Ranzi; P. Gaffuri; T. Faravelli; P. Dagaut, *A wide-range modeling study of n-heptane oxidation*, Combustion and flame 103 (1) (1995) 91-106
26. J. Bugler; K. P. Somers; E. J. Silke; H. J. Curran, *Revisiting the Kinetics and Thermodynamics of the Low-Temperature Oxidation Pathways of Alkanes: A Case Study of the Three Pentane Isomers*, The Journal of Physical Chemistry A (2015)
27. E. Ranzi; M. Dente; A. Goldaniga; G. Bozzano; T. Faravelli, *Lumping procedures in detailed kinetic modeling of gasification, pyrolysis, partial oxidation and combustion of hydrocarbon mixtures*, Progress in Energy and Combustion Science 27 (1) (2001) 99-139
28. E. Ranzi; A. Frassoldati; S. Granata; T. Faravelli, *Wide-range kinetic modeling study of the pyrolysis, partial oxidation, and combustion of heavy n-alkanes*, Industrial & engineering chemistry research 44 (14) (2005) 5170-5183
29. M. Dente; E. Ranzi; A. Goossens, *Detailed prediction of olefin yields from hydrocarbon pyrolysis through a fundamental simulation model (SPYRO)*, Computers & Chemical Engineering 3 (1) (1979) 61-75
30. E. Ranzi; M. Dente; T. Faravelli; G. Pennati, *Prediction of kinetic parameters for hydrogen abstraction reactions*, Combustion science and technology 95 (1-6) (1993) 1-50
31. E. Ranzi; A. Frassoldati; A. Stagni; M. Pelucchi; A. Cuoci; T. Faravelli, *Reduced Kinetic Schemes of Complex Reaction Systems: Fossil and Biomass-Derived Transportation Fuels*, International Journal of Chemical Kinetics 46 (9) (2014) 512-542
32. A. Sudholt, L. Cai, J. Heyne, F.M. Haas, H. Pitsch, F.L. Dryer *"Ignition characteristics of a bio-derived class of saturated and unsaturated furans for engine applications."* *Proceedings of the Combustion Institute* 35.3 (2015): 2957-296
33. K.P. Somers, J.M. Simmie, F. Gillespie, U. Burke, J. Connoly, W.K. Metcalfe, F. Battin-Leclerc, P. Dirrenberger, O. Herbinet, P.A. Glaude, H.J. Curran "A high temperature and atmospheric pressure experimental and detailed chemical kinetic modelling study of 2-methyl furan oxidation." *Proceedings of the Combustion Institute* 34.1 (2013): 225-232.
34. J.M. Simmie "Kinetics and thermochemistry of 2, 5-dimethyltetrahydrofuran and related oxolanes: next next-generation biofuels." *The Journal of Physical Chemistry A* 116.18 (2012): 4528-4538.
35. L. A. Curtiss; P. C. Redfern; K. Raghavachari, *Gaussian-4 theory using reduced order perturbation theory*, The Journal of chemical physics 127 (12) (2007) 124105

36. M. Frisch; G. Trucks; H. Schlegel; G. Scuseria; M. Robb; J. Cheeseman; G. Scalmani; V. Barone; B. Mennucci; G. Petersson, in Gaussian 09, Version A.01 (2009).
37. K.P. Somers and J. M. Simmie. "*Benchmarking Compound Methods (CBS-QB3, CBS-APNO, G3, G4, W1BD) against the Active Thermochemical Tables: Formation Enthalpies of Radicals*." The Journal of Physical Chemistry A 119.33 (2015): 8922-8933.
38. V. B. Oyeyemi; D. B. Krisiloff; J. A. Keith; F. Libisch; M. Pavone; E. A. Carter, *Size-extensivity-corrected multireference configuration interaction schemes to accurately predict bond dissociation energies of oxygenated hydrocarbons*, The Journal of chemical physics 140 (4) (2014) 044317
39. V. B. Oyeyemi; J. A. Keith; E. A. Carter, *Trends in Bond Dissociation Energies of Alcohols and Aldehydes Computed with Multireference Averaged Coupled-Pair Functional Theory*, The Journal of Physical Chemistry A 118 (17) (2014) 3039-3050
40. V. B. Oyeyemi; J. A. Keith; E. A. Carter, *Accurate bond energies of biodiesel methyl esters from multireference averaged coupled-pair functional calculations*, The Journal of Physical Chemistry A 118 (35) (2014) 7392-7403
41. B. Ruscic, *Uncertainty Quantification in Thermochemistry, Benchmarking Electronic Structure Computations, and Active Thermochemical Tables*. Int. J. Quantum Chem. 114, 1097-1101 (2014).
42. P.J. Linstrom and W.G. Mallard, Eds., *NIST Chemistry WebBoo*k, NIST Standard Reference Database Number 69, National Institute of Standards and Technology, Gaithersburg MD, 20899, http://webbook.nist.gov, (retrieved August 12, 2016).

43. H.-H. Carstensen; A. M. Dean in: *Development of detailed kinetic models for the thermal conversion of biomass via first principle methods and rate estimation rules*, ACS Symposium Series, 2010; 2010; pp 201-243.
44. A. Frassoldati; R. Grana; T. Faravelli; E. Ranzi; P. Oßwald; K. Kohse-Höinghaus, *Detailed kinetic modeling of the combustion of the four butanol isomers in premixed low-pressure flames*, Combustion and flame 159 (7) (2012) 2295-2311
45. G. da Silva; J. W. Bozzelli; L. Liang; J. T. Farrell, *Ethanol oxidation: Kinetics of the α-hydroxyethyl radical+ O2 reaction*, The Journal of Physical Chemistry A 113 (31) (2009) 8923-8933
46. M. Pelucchi; E. Ranzi; A. Frassoldati; T. Faravelli, *Alkyl radicals rule the low temperature oxidation of aldehydes*, Proceedings of the Combustion Institute 36 (2016) accepted.
47. R. Grana; A. Frassoldati; A. Cuoci; T. Faravelli; E. Ranzi, *A wide range kinetic modeling study of pyrolysis and oxidation of methyl butanoate and methyl decanoate. Note I: Lumped kinetic model of methyl butanoate and small methyl esters*, Energy 43 (1) (2012) 124-139
48. M. H. Hakka; H. Bennadji; J. Biet; M. Yahyaoui; B. Sirjean; V. Warth; L. Coniglio; O. Herbinet; P.-A. Glaude; F. Billaud, Oxidation of methyl and ethyl butanoates, International Journal of Chemical Kinetics 42 (4) (2010) 226-252
49. J. Mendes, C.-W. Zhou, H. J. Curran. "*Theoretical Study of the Rate Constants for the Hydrogen Atom Abstraction Reactions of Esters with• OH Radicals."* The Journal of Physical Chemistry A 118.27 (2014): 4889-4899.
50. T. Tan, X. Yang, Y. Ju, E.A. Carter "Ab initio kinetics studies of hydrogen atom abstraction from methyl propanoate." Physical Chemistry Chemical Physics 18.6 (2016): 4594-4607.
51. Lam, K.-Y.; Davidson, D. F.; Hanson, R. K. High-Temperature Measurements Of The Reactions Of • OH With Small Methyl Esters: Methyl Formate, Methyl Acetate, Methyl Propanoate, And Methyl Butanoate. J. Phys. Chem. A 2012, 116, 12229−12241
52. D. Felsmann, H. Zhao, Q. Wang, I. Graf, T. Tan, X. Yang, E.A. Carter, Y. Ju, K. Kohse-Hoingaus *Contributions to improving small ester combustion chemistry: Theory, model and experiments.* Proceedings of the Combustion Institute (2016). In press, doi:10.1016/j.proci.2016.05.012
53. S. Gaïl; M. J. Thomson; S. M. Sarathy; S. A. Syed; P. Dagaut; P. Diévart; A. J. Marchese; F. L. Dryer, A wide-ranging kinetic modeling study of methyl butanoate combustion, Proceedings of the Combustion Institute 31 (1) (2007) 305-311
54. S. Walton; M. Wooldridge; C. Westbrook, An experimental investigation of structural effects on the auto-ignition properties of two C 5 esters, Proceedings of the Combustion Institute 32 (1) (2009) 255-262

55. R. Grana, A. Frassoldati, C. Saggese, T. Faravelli, E. Ranzi *A wide range kinetic modeling study of pyrolysis and oxidation of methyl butanoate and methyl decanoate–Note II: Lumped kinetic model of decomposition and combustion of methyl esters up to methyl decanoate.* Combustion and Flame, 159(7), (2012). 2280-2294.
56. A. Rodriguez, O. Herbinet, F. Battin-Leclerc, A. Frassoldati, T. Faravelli, E. Ranzi *Experimental and modeling investigation of the effect of the unsaturation degree on the gas-phase oxidation of fatty acid methyl esters found in biodiesel fuels*. Combustion and Flame, 164, (2016) 346-362.
57. E. Ranzi; T. Faravelli; P. Gaffuri; G. Pennatti; A. Sogaro, A wide range modeling study of propane and n-butane oxidation, Combustion science and technology 100 (1-6) (1994) 299-330
58. E. Ranzi; C. Cavallotti; A. Cuoci; A. Frassoldati; M. Pelucchi; T. Faravelli, New reaction classes in the kinetic modeling of low temperature oxidation of n-alkanes, Combustion and flame 162 (5) (2015) 1679-1691
59. O. Herbinet; F. Battin-Leclerc; S. Bax; H. Le Gall; P.-A. Glaude; R. Fournet; Z. Zhou; L. Deng; H. Guo; M. Xie; F. Qi, Detailed product analysis during the low temperature oxidation of n-butane, Physical Chemistry Chemical Physics 13 (1) (2011) 296-308
60. D. Healy; N. Donato; C. Aul; E. Petersen; C. Zinner; G. Bourque; H. Curran, n-Butane: Ignition delay measurements at high pressure and detailed chemical kinetic simulations, Combustion and flame 157 (8) (2010) 1526-1539
61. A. Cuoci; A. Frassoldati; T. Faravelli; E. Ranzi, OpenSMOKE++: An object-oriented framework for the numerical modeling of reactive systems with detailed kinetic mechanisms, Computer Physics Communications 192 (2015) 237-264
62. R. Grana; A. Frassoldati; T. Faravelli; U. Niemann; E. Ranzi; R. Seiser; R. Cattolica; K. Seshadri, *An experimental and kinetic modeling study of combustion of isomers of butanol*, Combustion and flame 157 (11) (2010) 2137-2154
63. K. Heufer; R. Fernandes; H. Olivier; J. Beeckmann; O. Röhl; N. Peters, *Shock tube investigations of ignition delays of n-butanol at elevated pressures between 770 and 1250K*, Proceedings of the Combustion Institute 33 (1) (2011) 359-366
64. S. Vranckx; K. Heufer; C. Lee; H. Olivier; L. Schill; W. Kopp; K. Leonhard; C. Taatjes; R. Fernandes, *Role of peroxy chemistry in the high-pressure ignition of n-butanol–Experiments and detailed kinetic modelling*, Combustion and flame 158 (8) (2011) 1444-1455
65. B. W. Weber; K. Kumar; Y. Zhang; C.-J. Sung, *Autoignition of n-butanol at elevated pressure and low-to-intermediate temperature*, Combustion and flame 158 (5) (2011) 809-819
66. S. Le Calvé; D. Hitier; G. Le Bras; A. Mellouki, *Kinetic studies of OH reactions with a series of ketones*, The Journal of Physical Chemistry A 102 (24) (1998) 4579-4584
67. N. Sebbar; J. W. Bozzelli; H. Bockhorn, *Thermochemistry and Kinetics for 2-Butanone-3yl Radical (CH3C (= O) CH• CH3) Reactions with O2*, Zeitschrift für Physikalische Chemie International journal of research in physical chemistry and chemical physics 225 (9-10) (2011) 993-1018
68. N. Sebbar; J. Bozzelli; H. Bockhorn, *Thermochemistry and Kinetics for 2-Butanone-1-yl Radical (CH2· C (= O) CH2CH3) Reactions with O2*, The Journal of Physical Chemistry A 118 (1) (2013) 21-37
69. K.-Y. Lam; D. F. Davidson; R. K. Hanson, *High-Temperature Measurements of the Reactions of OH with a Series of Ketones: Acetone, 2-Butanone, 3-Pentanone, and 2-Pentanone*, The Journal of Physical Chemistry A 116 (23) (2012) 5549-5559
70. K.-Y. Lam; W. Ren; S. H. Pyun; A. Farooq; D. F. Davidson; R. K. Hanson, *Multi-species time-history measurements during high-temperature acetone and 2-butanone pyrolysis*, Proceedings of the Combustion Institute 34 (1) (2013) 607-615
71. J. Badra; A. E. Elwardany; F. Khaled; S. S. Vasu; A. Farooq, *A shock tube and laser absorption study of ignition delay times and OH reaction rates of ketones: 2-Butanone and 3-buten-2-one*, Combustion and Flame 161 (3) (2014) 725-734
72. Z. Serinyel; G. Black; H. Curran; J. Simmie, *A shock tube and chemical kinetic modeling study of methy ethyl ketone oxidation*, Combustion Science and Technology 182 (4-6) (2010) 574-587
73. M. Heiko, U. Burke, and K. A. Heufer. "*An experimental and theoretical comparison of C 3–C 5 linear ketones.*" Proceedings of the Combustion Institute (2016), in press doi:10.1016/j.proci.2016.05.050

74. C.-W. Zhou, J. M. Simmie, H. J. Curran. "*Ab initio and kinetic study of the reaction of ketones with ȮH for T= 500–2000 K. Part I: hydrogen-abstraction from H 3 CC (O) CH3–x (CH 3) x, x= 0↦2*." Physical Chemistry Chemical Physics 13.23 (2011): 11175-11192.

75. J.W. Allen, A.M. Scheer, C.W. Gao, S.S. Merchant, S.S. Vasu, O. Welz, J.D. Savee, D.L. Osborn, C. Lee, S. Vranckx, Z. Wang, F. Qi, R.X. Fernandes, W.H. Green, M.Z. Hadi, C.A. Taatjes "*A coordinated investigation of the combustion chemistry of diisopropyl ketone, a prototype for biofuels produced by endophytic fungi*." Combustion and Flame 161.3 (2014): 711-724.

76. K. HadjAli; M. Crochet; G. Vanhove; M. Ribaucour; R. Minetti, *A study of the low temperature autoignition of methyl esters*, Proceedings of the Combustion Institute 32 (1) (2009) 239-246

77. S. Gaïl; S. Sarathy; M. Thomson; P. Diévart; P. Dagaut, *Experimental and chemical kinetic modeling study of small methyl esters oxidation: Methyl (E)-2-butenoate and methyl butanoate*, Combustion and flame 155 (4) (2008) 635-650

78. K. Heufer; J. Bugler; H. Curran, *A comparison of longer alkane and alcohol ignition including new experimental results for n-pentanol and n-hexanol*, Proceedings of the Combustion Institute 34 (1) (2013) 511-518

79. A. Rodriguez, O. Herbinet, F. Battin-Leclerc. "*A study of the low-temperature oxidation of a long chain aldehyde: n-hexanal.*" Proceedings of the Combustion Institute (2016), in press, doi:10.1016/j.proci.2016.05.047

80. K.C. Lin, J.Y. Lai, A. Violi. "*The role of the methyl ester moiety in biodiesel combustion: A kinetic modeling comparison of methyl butanoate and n-butane*." Fuel 92.1 (2012): 16-26.

81. S.J. Klippenstein, Proceedings of the Combustion Institute (2016), in press.